

Sub and Near Barrier Fusion of Neutron Rich Heavy Nuclei - Studies with Radioactive Ion Beams

D. Shapira¹

¹ Physics Division, Oak Ridge National Laboratory, Oak Ridge, TN 37831, USA

² the second here

Received: date / Revised version: date

Abstract. The availability of accelerated fission fragments at HRIBF allows us to study fusion reactions where one of the reactants is a short-lived exotic nucleus. Most interesting in this respect are entrance channels involving neutron rich targets and projectile - where enhanced survival probability of the compound system may allow the synthesis of heavier system. Much depends though on the dynamic evolution of the captured nuclei into a compound nucleus and the ensuing competition between fission and evaporation residue decay modes. Our studies of fusion between heavy neutron-rich nuclei are aimed at acquiring data that will lead to the understanding and eventually the ability to predict the probabilities for these different processes.

PACS. 24.10.-i Nuclear reaction models and methods – 25.60.-t Reactions induced by unstable nuclei – 25.60.Pj Fusion reactions

1 Introduction

Nucleus nucleus capture is a precondition to their fusion and the use of neutron rich nuclei increases stability of the formed compound against fission. While the projected intensity of radioactive beam species is much diminished compared to stable nuclei, it may be that a large enhancement in capture probability combined with the population of a more neutron rich composite nucleus will allow the synthesis of new heavy elements. At the HRIBF we address the question of enhancement in nucleus-nucleus capture for neutron rich species by combining accelerated neutron rich products from proton or deuteron induced fission of U with neutron rich targets. We hope to study the role extra neutrons may play in enhancing the probability of nucleus nucleus capture. Fig. 1 shows the large span of Sn isotopes available, of these the squares (red on line) show radioactive Sn isotopes. Some of the radioactive Sn isotopes are already available and accelerated at HRIBF [1]. ^{132}Sn is available in almost pure form at intensities nearing $10^5/\text{sec}$. Accelerated ^{134}Sn ions are delivered with other $A=134$ isobaric contaminants at expected rate of about 500/sec (for ^{134}Sn). The study of weak processes such as sub-barrier fusion at low beam intensities poses a challenge. The following section will present the system we developed for these studies. Results of some of our measurements are presented next. We also attempt to account for the level of capture cross section observed in the sys-

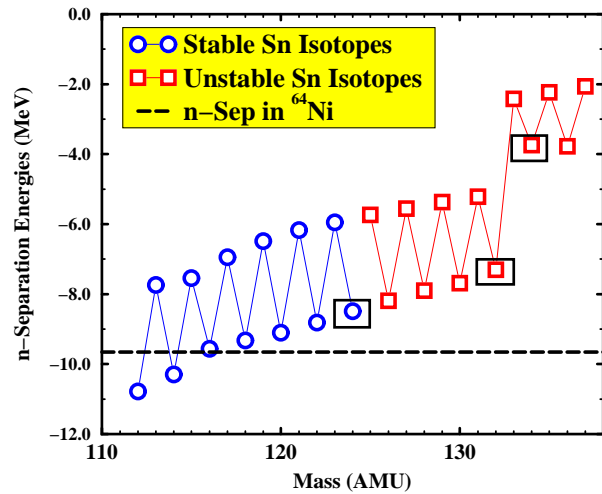


Fig. 1. Neutron separation energies of Sn isotopes. The neutron separation energy from ^{64}Ni is also indicated

tem studied so far and examine what systems would be appropriate for future studies.

2 Description of the experimental system

A schematic block diagram of the system is shown in Fig. 2 part A. Among its special feature is the ability to sample

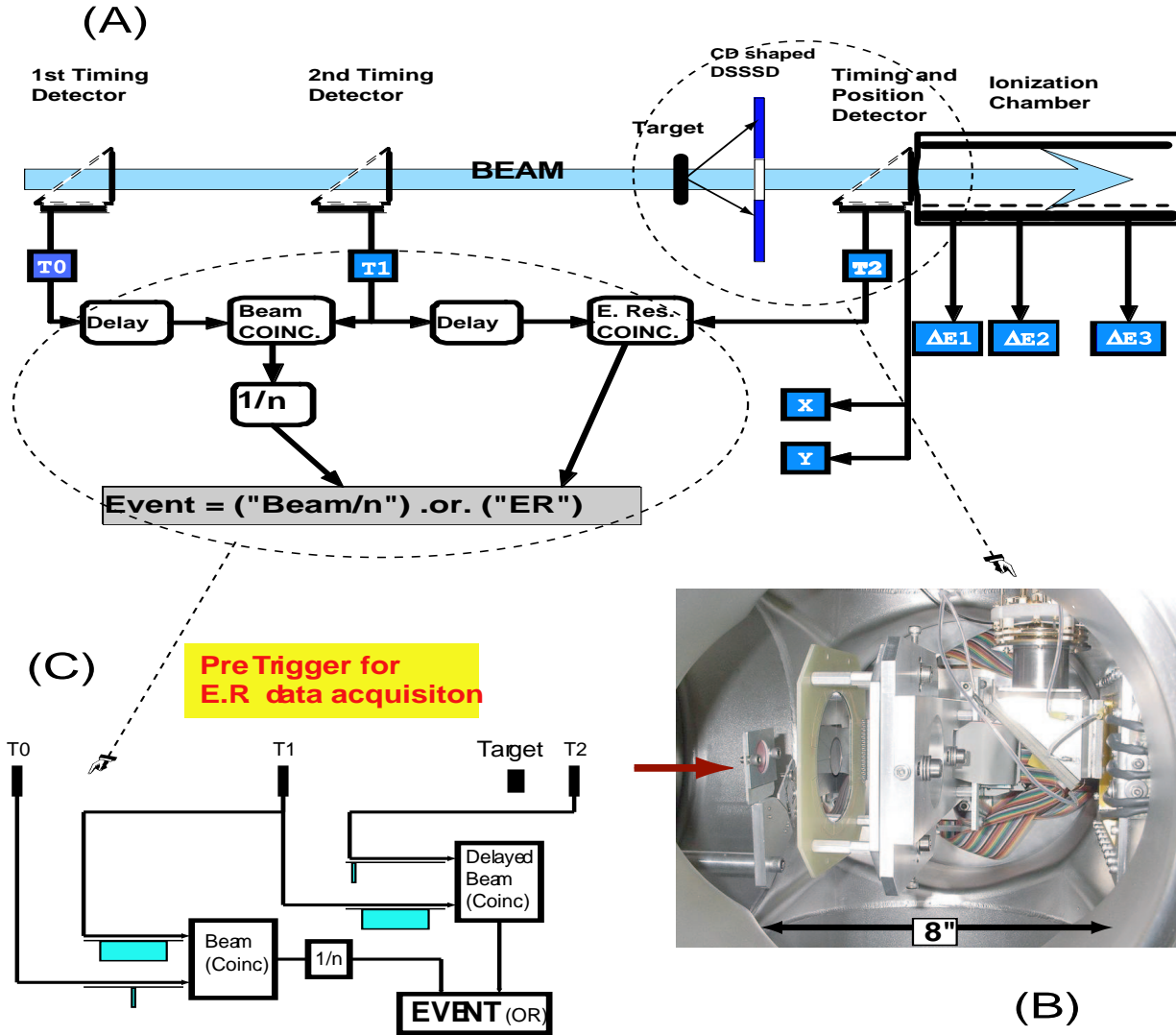


Fig. 2. A - schematic diagram of the experimental setup. B - a photograph of the area encircled in part A. C - the pre-trigger logic.

the beam and its components in the ionization chamber. The pre trigger allows us to count the ER events with minimal dead time of the data acquisition system. We also placed a CD shaped double-sided silicon strip detector close to the target allowing for coincidence detection of non elastic two body events from the reaction. The efficiency for evaporation residue detection is near 100% for inverse kinematics and near 5% for fission fragment detection. A detailed description of this system has been published [2]. Part B of Fig. 2 is a photograph of this compact system, packed inside an 8" six-way cross. The pre-trigger logic that allows for a $1/n$ sample of the beam is shown in part C of the same figure.

3 Measured Evaporation Residue and Fission Cross Sections

Fig. 3 shows the evaporation residue cross sections for three isotopes of Sn on a ^{64}Ni target. The ^{124}Sn data were

taken for comparison with other evaporation residue data measured for the same system [3]. More detail on these measurements can be found in [2]. The ^{132}Sn ER data were published [4] but the ^{134}Sn data are new. It can be seen that the $^{134}\text{Sn} + ^{64}\text{Ni} \rightarrow \text{ER}$ data set is yet incomplete. We have indicated with a dashed vertical line the two energies where we plan to acquire more data which we consider is a minimum amount of data required to be able to draw some conclusion about the behavior of this system. Most interesting would be the data below the barrier where we expect contribution from fission to be small and we can see if the slope of the excitation function is similar to the other two systems shown in Fig. 3.

Fig. 4 highlights some of the difficulties encountered in measuring the ^{134}Sn data set. ^{134}Sn appears only as one component in a mixture of different isobars. This is the situation when we extract sulfides ($A=166$) from the ion source. The ^{134}Ba does not pose a problem at energies near and below the $^{134}\text{Sn} + ^{64}\text{Ni}$ barrier. The ^{134}Te beam is

Distribution of A=134 Isobars in beam varies.

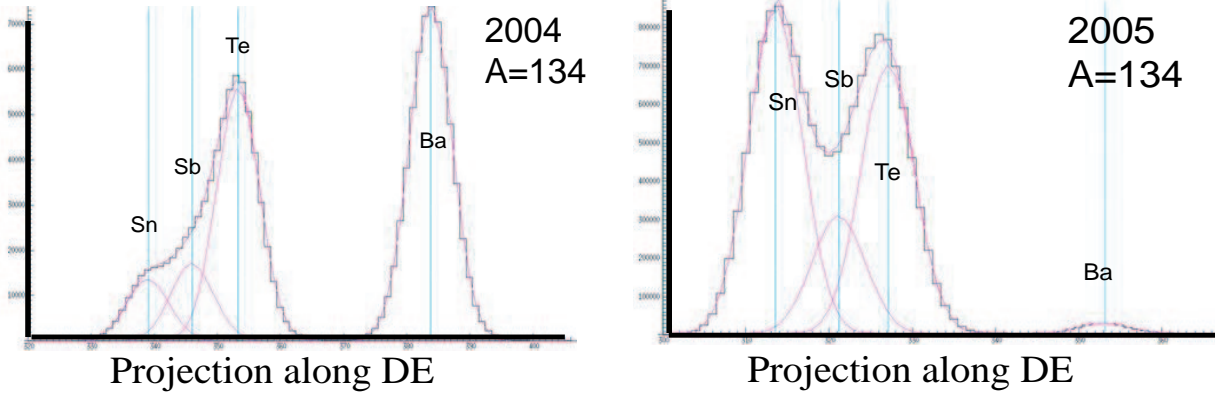


Fig. 4. Isobars mixture for A=134 delivered following the extraction of mass 166 (sulfides) from the ion source

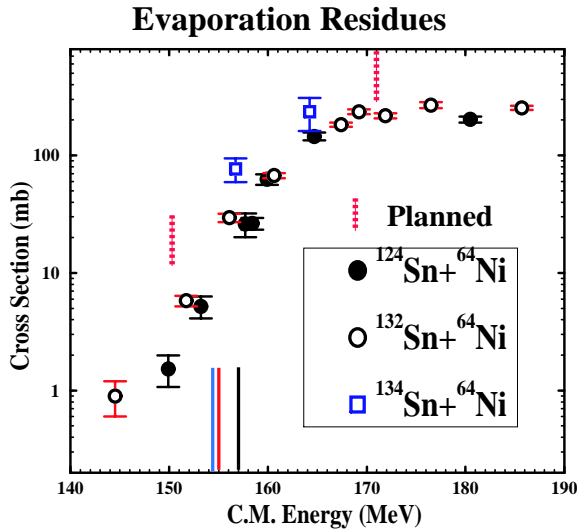


Fig. 3. Evaporation residue data for several Sn isotopes on ^{64}Ni

available with high purity when we extract mass 134 out of the ion source. What we did is measure the cross section for ER production in $^{134}\text{Te}+^{64}\text{Ni}$ collisions. The data for $^{134}\text{Te}+^{64}\text{Ni}\rightarrow\text{ER}$ were taken at the same bombarding energies and with the same target which were used in the measurements of ERs with the isobar mixture. Since we constantly are able to monitor and get the exact count for beam particles of each isobar in the mixture, we can subtract the $^{134}\text{Te}+^{64}\text{Ni}\rightarrow\text{ER}$ contribution from the combined ER yield measured with the mixed beam. Separating the ^{134}Sn and ^{134}Sb contribution is more involved. As can be seen in Fig. 4 the ratio of ^{134}Sn to ^{134}Sb in the beam varies with time. It should then be possible to untangle the two cross sections using two sets of ER data obtained with a different ratio of ^{134}Sn to ^{134}Sb in the beam. To attain an accuracy of 10 then 200 ER counts in

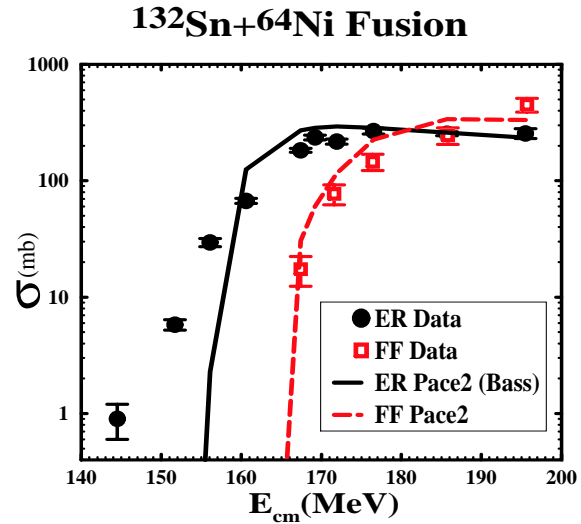


Fig. 5. Evaporation residues and Fission following fusion of $^{132}\text{Sn}+^{64}\text{Ni}$. Also shown are the yields as predicted by the Statistical model Monte Carlo code PACE2 [5]

total (assuming similar cross sections). This will require longer running time but will result in data on two systems.

With our present setup we can measure also the fission decay channel, though with much reduced efficiency. The beam intensity of ^{132}Sn (near $10^5/\text{s}$) was sufficient to allow a good measurement of $^{132}\text{Sn}+^{64}\text{Ni}\rightarrow\text{fusion-fission}$. Fig. 5 shows the fission data for this system. More details on this measurement are available in a separate contribution to this conference and in an upcoming paper [16]. In Fig. 5 we show the fission data and the evaporation residue yield from fusion $^{132}\text{Sn}+^{64}\text{Ni}$. It appears that at the 100mb level (near the barrier) the ER yield dominates the decay of the fused $^{132}\text{Sn}+^{64}\text{Ni}\rightarrow^{196}\text{Pt}$. One expects a similar situation for the decay of $^{134}\text{Sn}+^{64}\text{Ni}\rightarrow^{198}\text{Pt}$ which is even more neutron rich. At higher energies (more than 110% of the

interaction barrier) one must measure also the fission yield which at the present rate of ^{134}Sn beam intensity and purity is not feasible with our experimental setup.

4 WKB calculations of Sub-Barrier Capture Cross Sections

The experiments we embarked on are aimed at finding if there is a large enhancement of nucleus-nucleus capture cross sections at sub-barrier energies due to large neutron excess in the entrance channel. What we are searching for is enhancement that goes beyond nuclear size effects. In this section we examine some semi-classical models that emphasize the role of neutron richness in the entrance channel may have on the nucleus-nucleus capture cross section.

4.1 Two step capture following neutron transfer and the neutron flow model

There are several models that predict enhancement of sub-barrier fusion well beyond size effects two of which we will examine now [7–10].

In his analysis of near and sub-barrier fusion data of several systems Stelson [7,8] found that the cross section has a parabolic dependence on bombarding energy. He has shown that such dependence arises from integrating the classical single barrier fusion cross section over a flat (constant) distributions of barriers. This flat barrier distribution has a threshold below the standard interaction barrier. Subsequent analysis associated the location of this threshold of the barrier distribution, to conditions where the valence neutron in one of the colliding nuclei is not bound to that nucleus [8,11]. Such a condition dubbed "neutron-flow" arise when the neutron wells of the two approaching nuclei overlap to a degree where the barrier between these wells gets depressed to a level below the separation energy of the valence neutron (see Fig. 6).

Another, more recent approach [9,10] is a two-step capture model wherein neutron transfer to a channel with positive Q-value precedes barrier penetration. Following such transfer the kinetic energy in the entrance channel gets elevated with respect to the barrier resulting in an increase (exponential) to the probability of penetrating the nucleus-nucleus barrier. Ref. [9] and [10] differ in technical detail but in both cases penetration through the nucleus-nucleus barrier is treated in a WKB like formalism.

We implemented a WKB code that calculates the cross section of two nuclei to get captured in the nucleus-nucleus potential well. In our code we follow the prescription suggested in Refs. [9,10] with the modifications listed below:

- We use global potentials derived from fits to a large body of fusion data [12] which also includes parameterization that incorporates the effect of a Gaussian barrier distribution arising from inelastic excitation and deformation in the entrance channel.

- The neutron transfer form factor we use in our calculations saturates at inter-nuclear distances where neutron flow [7] is initiated rather than at some arbitrary distance of closest approach.
- We do not use a parabolic approximation for the barrier. The WKB transmission through the combined nuclear+Coulomb+centrifugal barrier is calculated for each partial wave.
- We include in our two-step calculation neutron transfer channels to all channels with Q-values that do not exceed 10MeV in magnitude. The effect of channels with both positive and negative Q value channels is considered.

4.2 Comparison of WKB calculation to Data

Our two-step WKB calculation for $^{40}\text{Ca}+^{90,96}\text{Zr}$ [13,14] are shown in Fig. 7. There are two items worth noting:

- These data were fit by the authors of Ref. [12], yet the calculation labeled "Wilczynski SB" does not fit the $^{40}\text{Ca}+^{96}\text{Zr}$ data set. The reason for that is that the potential we use in our calculation is the global potential as suggested in Ref. [12] this results in potential parameters that differ somewhat from those obtained by fitting the data.
- The effect of including all neutron transfer channels (negative as well as positive Q values) is that capture probability may be diminished after allowing for two-step capture. This effect is most noticeable near and slightly above the barrier where transfer to channels with negative Q-values will push the energy of the system down below the barrier.

Fig. 8 shows a comparison of the two step calculations to data for $^{132}\text{Sn}+^{64}\text{Ni}$ as well as predicted behavior for $^{132}\text{Sn}+^{58}\text{Ni}$. We have also included a comparison to a coupled channel (CC) calculation done with the code CCFUS [15]. The potential used in these CC calculations is one that fit similar data ($^{124}\text{Sn}+^{58}\text{Ni}$) and has target and projectile excitation as well as neutron transfer coupled explicitly. Further details can be found at [16]. The WKB calculation uses the global potential parameter given in [12]. Note that the data for this system were not included in the set fit by ref. [12] when extracting the global potential parameters. There are no data yet for the system $^{132}\text{Sn}+^{58}\text{Ni}$ but the two-step WKB calculation predict a substantial sub-barrier enhancement in the capture cross section for that system. Fig. 9 shows two comparison of of the two-step WKB to the scant data existing for $^{134}\text{Sn}+^{64}\text{Ni}$. The data here are near barrier data and present only ER measurements. Note however that we do not expect a substantial contribution of fission yields (see Fig. 5). The two calculations shown differ in the neutron transfer form factor. In one a large radius parameter $R=1.40\times(A_p^{\frac{1}{3}}+A_p^{\frac{1}{3}})$ is taken as the point at which the transfer form factor saturates. In the second calculation the neutron transfer form factor saturates at the radius for which neutron flow would occur.

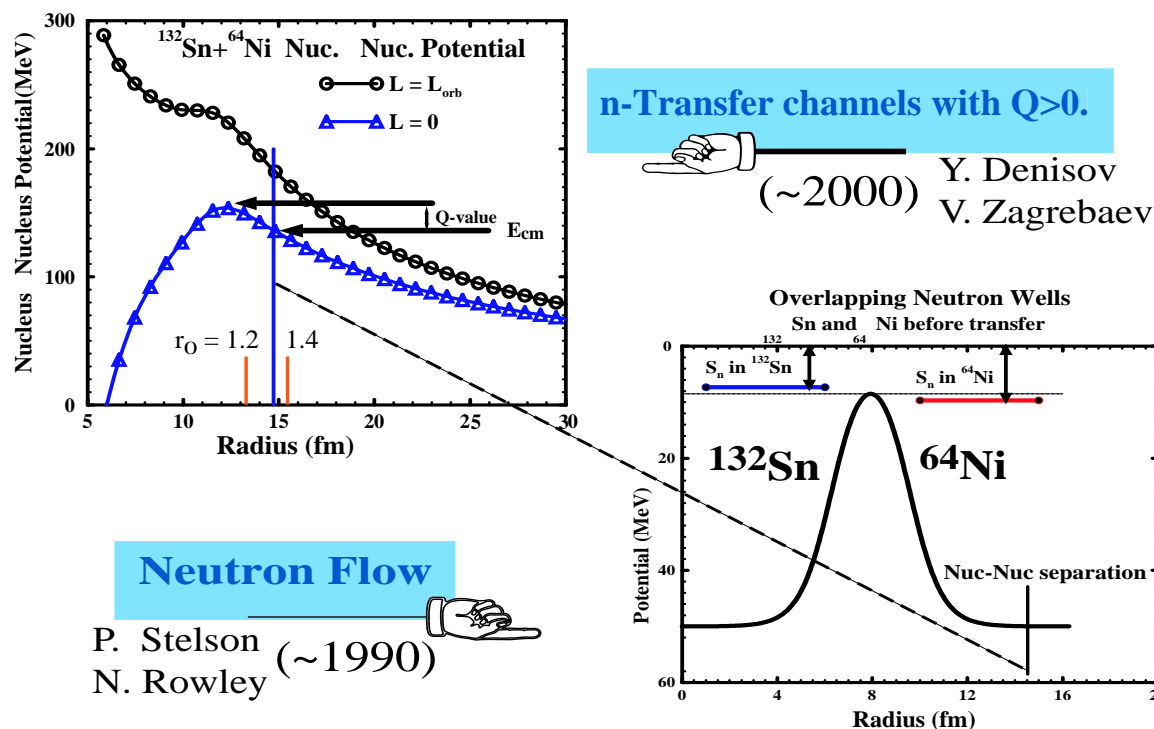


Fig. 6. Semi-classical models that associate capture cross section magnitude with the properties of neutron rich nuclei

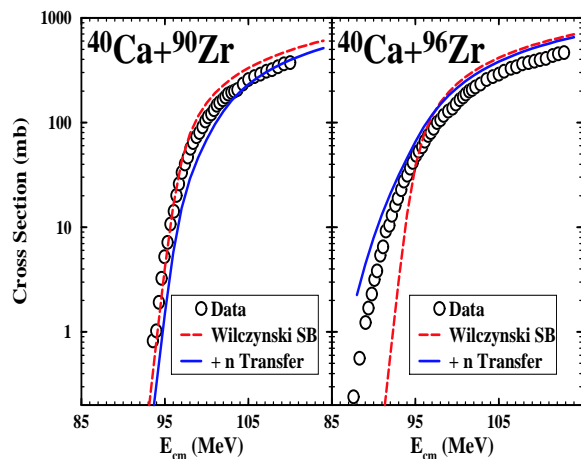


Fig. 7. Two-step WKB calculations for $^{40}\text{Ca} + ^{90,96}\text{Zr}$ data.

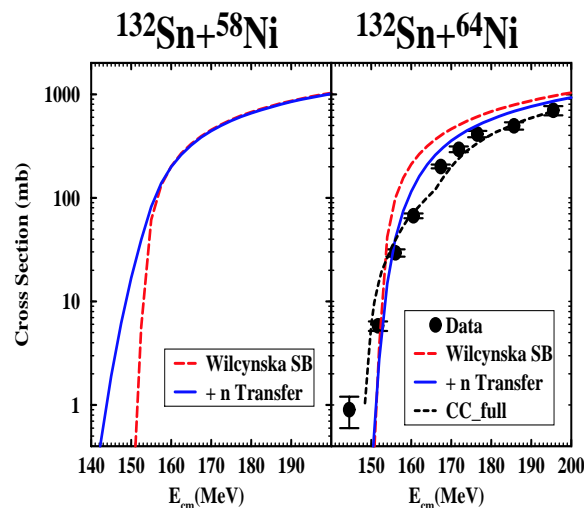


Fig. 8. Two-step WKB calculations for $^{132}\text{Sn} + ^{58,64}\text{Ni}$ systems.

5 Conclusion and outlook

We have begun to study the fusion of heavy very neutron-rich nuclei. The experimental setup designed for these measurements is ideal for detecting evaporation residues under reverse kinematics conditions. Clearly one could move to less asymmetric systems at the cost of some efficiency but the system is compact and simple to use and can yield reliable ER data in a few days of running with beam intensity ranging from 10^4 to 10^5 ions/sec. With better beam quality, quantity and purity this experimental setup, with some improvements, can be used to study a large number of reactions. As one moves to heavier and more highly charged systems fission will become the dom-

inant decay mode of the compound nucleus. Our present setup to study fission like decay has low efficiency and does not cover forward or backward angles (a ~ 15 degree cone). It is clear that in order to study capture for heavier system a new detection system that will have much higher efficiency for fission fragment detection and larger angle coverage will be needed. We have also explored the prediction of two semi-classical models dealing with the fusion or capture of two neutron rich nuclei. These simple models do fairly well in providing an order of magnitude estimate to sub-barrier fusion cross section. Clearly these models can

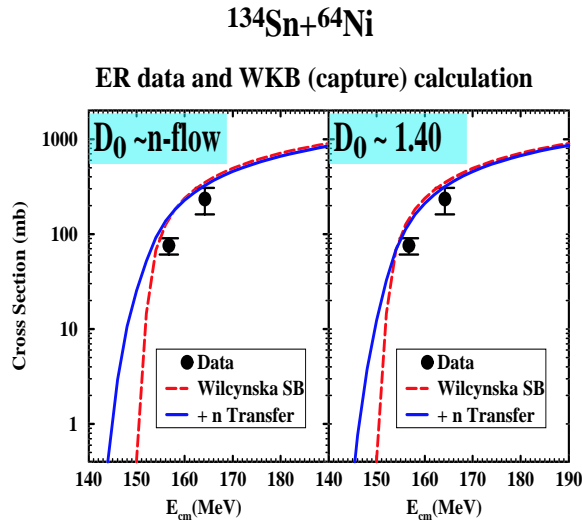


Fig. 9. Two-step WKB calculations for $^{134}\text{Sn}^{64}\text{Ni}$ data.

be improved. For example the optimum Q-value for neutron transfer is not exactly zero if neutrons are transferred from/to different orbitals. Also the probability of neutron transfer/flow should depend on the number of similar neutron in the sub-shell from which they are transferred (seniority). With further enrichment of the experimental data available such improvement to the model may also give a better description of the data and provide a more solid basis for predicting the behavior of systems that have not been measured yet. As data on more neutron-rich systems improve more sophisticated models may be developed. It is not clear if CC calculations are best at describing the states of two heavy nuclei that overlap already at large inter-nuclear distances or that macroscopic models can account well for processes that involve tunneling under the barrier. It appears that we have just started on a long journey.

References

1. D. Stracener Nucl. Instr. and Meth. **B204**, (2003) 42.
2. Shapira et al. Nucl. Instr. and Meth. **A551**, (2005) 330.
3. W.S. Freeman et al. Phys. Rev. Lett. **50**, (1983) 1564.
4. F. J. Liang, D. Shapira, C. J. Gross, J. R. Beene, J. D. Bierman, A. Galindo-Uribarri, J. Gomez del Campo, P. A. Hausladen, Y. Larochele, W. Loveland, P. E. Mueller, D. Peterson, D. C. Radford, D. W. Stracener and R. L. Varner Phys. Rev. Lett. **91**, (2003) 152701.
5. A. Gavron, Phys. Rev. C **21**, (1980) 230.
6. F. J. Liang et al. contribution to this conference. and F. J. Liang et al. to be published.
7. P.H. Stelson Phys. Lett. **B205**, (1988) 190.
8. P.H. Stelson et. al. Phys. Rev. C **41**, (1990) 1584.
9. V. Yu. Denisov Eur. Phys. J. **A7**, (2000) 87.
10. V. I. Zagrebaev, Phys. Rev. **C67**, (2003) 061601R.
11. N. Rowley, I. J. Thompson and M. A. Nagarajan Physics Lett. B **282**, (1992) 276.
12. K. Siwek-Wilczynska and J. Wilczynski Phys. Rev. **C69**, (2004) 024611.
13. G. Montagnoli, S. Beghini, F. Scarlassara, G. F. Segato, L. Corradi, C. J. Lin and A. M. Stefanini J. Phys. G **23**, (1997) 1341.
14. H. Timmers, D. Ackermann, S. Beghini, L. Corradi, J. H. He, G. Montagnoli, F. Scarlassara, A. M. Stefanini and N. Rowley, Nucl. Phys **A633**, (1998) 421.
15. K. Hagino, N. Rowley and A. T. Kruppa, Comput. Phys. Commun. **bf123**, (1999) 143.
16. F. Liang to be published in Proceedings of FUSION06 - AIP conference proceedings.